THIN-FILM SILICON SOLAR CELLS: STABILITY AND LIGHT TRAPPING

M. Zeman[1], G. van Elzakker[1], P. Sutta[2], O. Isabella[1], J. Krc[3]

[1]Delft University of Technology, PVMD /DIMES, Delft, Netherlands
[2]University of West Bohemia, NTRC, Plzeň, Czech Republic
[3] University of Ljubljana, Faculty of Electrical Engineering, Ljubljana, Slovenia

Key words: thin film silicon, stability, light trapping

Abstract: Thin-film silicon solar cell technology is one of the promising photovoltaic technologies for delivering low-cost solar electricity. Today the thin-film silicon PV market (402 MW$_p$ produced in 2008) is dominated by amorphous silicon based modules; however it is expected that the tandem amorphous/microcrystalline silicon mo-dules will take over in near future. The properties of silicon films grown from the mixture of hydrogen and silane will be discussed and the solar cell behavior will be presented. In order to increase the absorption in thin absorber layers novel approaches for photon management inside solar cells are developed. In this article i) optimal surface texture of the electrodes for introducing efficient light scattering and ii) development and implementation of optically-active layers for enhanced reflection at the back contact are presented.

Tankoplastne silicijeve sončne celice: Stabilnost in ujetje svetlobe

Kjučne besede: tankoplastni silicij, stabilnost, ujetje svetlobe

Izvleček: Tehnologija tankoplastnega silicija je ena izmed obetajočih tehnologij za proizvodnjo poceni električne energije. Na današnjem trgu fotovoltaike iz tankoplastnega silicija (proizvedenih 402 MW$_p$ v letu 2008) prevladujejo moduli iz amorfnega silicija, dasi se pričakuje, da bodo tandemske strukture amorfni/mikrokristalni silicij prevladovale v bližnji prihodnosti. V članku so obravnavane lastnosti silicijevih plasti narejene iz mešanice vodika in silana ter predstavljeno delovanje sončnih celic. Za povečevanje absorpcije v tanki absorpcijskih plasteh so razvite nove tehnike ujetja fotonov. V članku je predstavljena: i) optimalna teksturizacija elektrod za učinkovito sipanje svetlobe, ii) razvoj in uporaba optično aktivnih plasti za povečanje odbojnosti zadnje plasti.

1   Introduction

In 1975 Walter Spear and Peter LeComber reported that amorphous silicon had semiconducting properties. They demonstrated that the conductivity of amorphous silicon can be manipulated by several orders of magnitude by adding some phosphine or diborane gas to the glow discharge gas mixture /1/. This was a far-reaching discovery since until that time it had generally been thought that amorphous silicon could not be made n-type or p-type by substitutional doping. In fact, amorphous silicon suitable for electronic applica-tions, where doping is required, is an alloy of silicon and hydrogen. The electronic-grade amorphous silicon is therefore called hydrogenated amorphous silicon (a-Si:H).

The successful doping of amorphous silicon created tremendous interest in this material for two reasons. First, the material had several interesting properties that opened up many opportunities for semiconductor device applications. For example, due to the high absorption coefficient of a-Si:H in the visible range of the solar spectrum, a 1 mm thick a-Si:H layer is sufficient to absorb 90% of the usable solar energy. Second, the glow discharge deposition technique, also referred to as plasma enhanced chemical vapour deposition (PECVD), enabled the production of a-Si:H films over a large area (larger than 1 m^2) and at a low temperature (100°C to 400°C). The low processing tempera-ture allows the use of a wide range of low-cost substrates such as a glass sheet, a metal or a polymer foil. The a-Si:H is simply doped and alloyed by adding appropriate gases to a source gas, usually silane. These features have made a-Si:H a promising candidate for low-cost thin-film solar cells.

The first a-Si:H solar cell was made by Carlson and Wronski in 1976 and exhibited an energy conversion efficiency of 2.4% /2/. The University of Neuchâtel introduced a micromorph tandem solar cell in 1994, which comprised an a-Si:H top cell and a hydrogenated microcrystalline silicon (μc-Si:H) bottom cell /3/. Thin-film silicon solar cell technology has improved considerably, and today, it is capable of producing solar cells with initial efficiencies exceeding 15% /4/. It has also matured as production technology that delivered modules with a total output power of 402 MW$_p$ in 2008 /5/. Based on the companies' announcements the production capacity of thin-film silicon modules is expected to grow to almost 8 GW in the year 2010. The thin-film silicon PV market is dominated by amorphous silicon based modules; however it is expected that the micromorph tandem modules will take over in near future. Two manufacturing methods for thin film silicon solar cells can be distinguished; the silicon-on-glass approach and the roll-to-roll approach, in which solar cells are deposited on flexible substrates.

A drawback of the a-Si:H silicon solar cell technology is a relatively low stabilized efficiency of modules that varies between 5 to 8%. A challenge of this technology is to suppress the light-induced degradation of amorphous silicon solar cells. A widely used method for obtaining more stable a-Si:H material is based on applying hydrogen dilution of silane during its growth. In this article the properties of silicon films grown from the mixture of hydrogen and silane are discussed and the performance of solar cells with hydrogen diluted absorber layers is presented.

An efficient utilization of the sun spectrum is a key issue in the field of thin-film silicon solar cell technology. The tandem approach employing the combination of amorphous silicon and microcrystalline silicon absorber layers offers an improved performance of the modules reaching efficiencies above 10%. The tandem approach allows using thinner absorber layers in the component cells that contributes to a suppression of light induced degradation of a-Si:H component cell. When applying thinner absorber layers photon management becomes very important for increasing the absorption in the absorber layers. In this article two novel approaches for photon management are discussed: i) optimal surface texture of the substrates for introducing efficient light scattering and ii) development and implementation of optically-active layers based on 1-D photonic crystals for enhanced reflection at the back contact.

2 Improved stability of a-Si:H films

It has been demonstrated that solar cells with a-Si:H absorber layers prepared from silane diluted with hydrogen in plasma-enhanced chemical vapor deposition (PECVD) showed less degradation during light exposure than solar cells with undiluted absorbers /6,7/. This a-Si:H material is referred to as protocrystalline silicon (pc-Si:H) due to the fact that it will eventually evolve from the amorphous to microcrystalline phase when grown to a sufficient thickness /8,9/.

2.1 Experimental details

Individual hydrogenated silicon films and solar-cell absorber layers were deposited under the following deposition conditions; an rf-power of 4 W, a silane (SiH_4) flow of 5 sccm, a substrate temperature of 180°C. The hydrogen dilution is expressed by the dilution ratio R, which is defined as $R=/H_2///SiH_4/$. The dilution was varied between R > 0 and R = 40. An undiluted reference film (R = 0) was grown at a different pressure of 0.7 mbar and a SiH_4 flow of 40 sccm. The thickness of all films was ~ 300 nm, which corresponds to the thickness of the absorber layer in solar cells. In order to obtained 300 nm thick pc-Si:H films at all R the chamber pressure of 2.6 mbar was used. The individual films were deposited on Corning Eagle 2000 type glass substrates and on crystalline silicon (c-Si) substrates coated with a 20 nm thick a-Si:H layer grown from pure silane.

Single junction p-i-n solar cells were deposited on Asahi U-type substrates using the above described films as the absorber layers. The solar cells have the following structure: p-type a-SiC:H layer (10 nm)/a-SiC:H buffer layer/ intrinsic absorber layer (300 nm)/n-type a-Si:H layer (20 nm). The back contact consists of 300 nm aluminum. The external parameters of the solar cells (efficiency ç, fill factor ff, short-circuit current density J_{SC}, open-circuit voltage V_{OC}) were determined from I-V measurements using an Oriel Corporation solar simulator. The solar cells were degraded at a constant temperature of 50 şC with halogen lamps using a power density of 100 mW/cm^2.

The structural properties of the films were studied by X-ray diffraction (XRD) analysis using an automatic powder diffractometer X'pert Pro in asymmetric goniometer configurations with CuK-alpha radiation (lambda = 0.154 nm).

2.2 Structural properties of a-Si:H films

The XRD technique was used to study the influence of hydrogen dilution of silane on the structural properties of pc-Si:H films. In particular the narrowing of the first scattering peak (FSP) in the XRD spectra was investigated since this parameter is used as an indication of an improved medium range order (MRO). Figure 1 shows the FSP of the pc-Si:H film prepared at R=20. The procedure to obtain this XRD pattern is described elsewhere /10/.It was found that the FSP peak of all films of the dilution series could be fitted with a large-area peak centered around 27.5 degrees and a smaller peak centered around 32.5 degrees. In figure 1 the XRD patterns for crystalline silicon (Si) and crystalline silicon hydride (Si_4H) standards are included.. Comparing the standards to the measured XRD patterns we find a striking match between the position of the two Pearson VII functions and the silicon hydride lines, while the silicon (111) line clearly does not correspond to the center position at 27.5 degrees. Given the controversy regarding the origin of the a-Si:H FSP /11/, this result provides an interesting new interpretation of the ordered domains in the amorphous matrix. A good agreement between the position of the peaks of the measured lines and the standard XRD patterns of the silicon hydride provides evidence that the diffracting signal comes mainly from ordered domains of a tetragonal silicon-hydride /12/ and not from ordered domains of silicon.

The dominant peak at 27.5 degrees was used for the further analysis of the structural properties. Figure 2 shows the FWHM values of this peak as a function of R. The figure demonstrates that the FWHM decreases with increasing R from 0 to 20, and remains nearly constant when R is further increased from R = 20 to R = 40. This confirms previous reports about the narrowing of the FSP /10/, but shows for the first time that this effect saturates for a certain value of R.
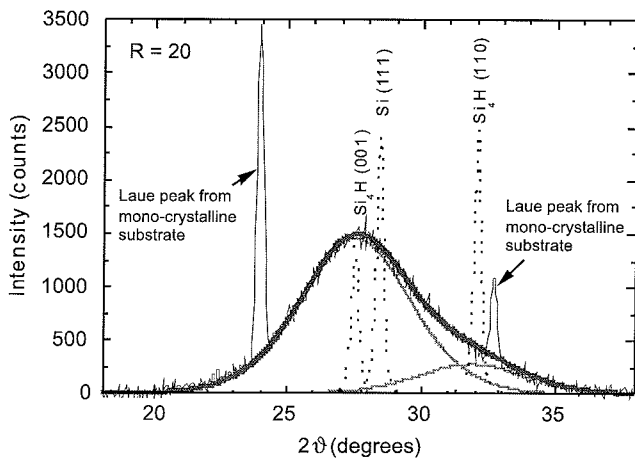
Fig. 1:   XRD patterns of the FSP measured on a 300
          nm thick pc-Si:H film deposited at R=20 on a
          c-Si substrate. Also shown are the XRD lines
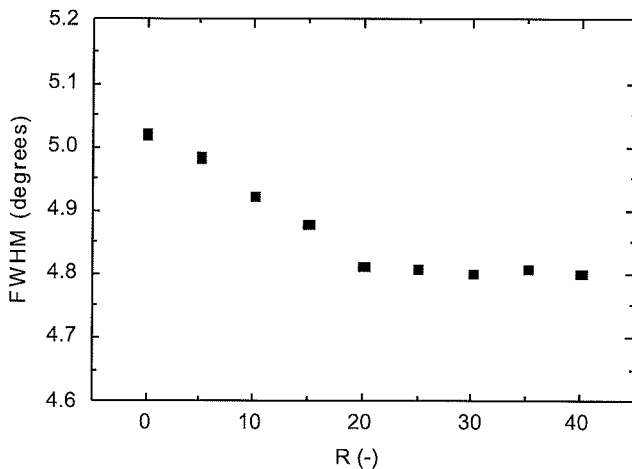   for crystalline Si and Si₄H standards.

Fig. 2:   FWHM values of the FSP as a function of R of
          the pc-Si:H films deposited on a c-Si substrate.

2.3 Degradation behavior of a-Si:H solar cells

The a-Si:H films prepared from hydrogen diluted silane were implemented as absorber layers in p-i-n solar cells. The solar cells were subjected to a degradation experiment. Figure 3 shows the evolution of the solar cell efficiency with the exposure time. In Fig. 3 the efficiency is normalized to the initial value before degradation. The degradation experiment confirms that the cells with absorber layers deposited using hydrogen dilution are more stable to light exposure. A clear reduction of the degradation is already observed when the dilution ratio is increased from R = 0 to R = 10 and the degradation is further suppressed when R is increased to 20. However, solar cells with absorber layers prepared at R > 20 exhibit similar degradation behavior as the cell with the absorber layer prepared at R = 20. The efficiency of the solar cells with absorber layers prepared at R ≥ 20 stabilizes at around 88% of their initial efficiency.

The similar degradation behavior of solar cells with absorber layers deposited at R ≥ 20 indicates that there is a correlation with the structural properties observed for the individual films. The saturation of the FWHM value of the FSP for pc-Si:H films prepared at R ≥ 20 is a strong indication that the structural order has achieved an optimal state in these films. The improved structural order contributes to suppressing the light induced degradation by de creasing the amount of weak Si-Si bonds which are removed by hydrogen etching of the growing surface /13/.
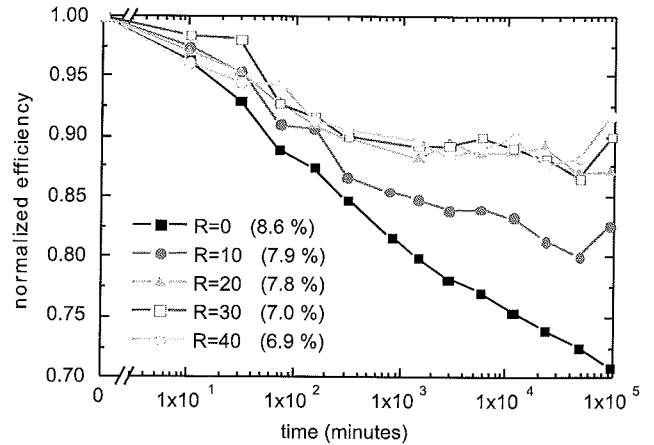

Fig. 3:   Normalized η of diluted a-Si:H solar cells as a
          function of illumination time. The initial values
          of η are given in brackets.

However, the improved structural order in amorphous films still does not prevent the occurrence of the degradation. The mechanisms that initiate the degradation have to be further investigated in order to fully prevent it.

3   Advanced light trapping

At present, further development and implementation of efficient light trapping is considered the most important research area in the field of thin-films silicon solar cells. Light-trapping techniques help to capture light in the desired parts of a solar cell, which are the absorber layers, and prevent it from escaping. Efficient light trapping in thin-films silicon solar cells is based on scattering of light at rough interfaces and the employment of high-reflective back contacts and refractive-index matching layers in order to manipulate reflection in the cell. Scattering of light at rough interfaces results in a longer average optical path through the absorber layers. Repeated reflection at the back and front contacts causes multiple passes of light through the absorber layer. These processes determine an efficient light confinement that substantially enhances light absorption in the absorber layer and increases the photocurrent of the solar cell. In the case of tandem devices, the challenge of light scattering is to optimize the absorption for the top and the bottom cells. Any pass of light from the front to the back contact of the cell is accompanied by an absorption loss in the metallic back contact.

Minimizing optical losses at the back side of the solar cells has become an important issue and in this sense engineering of dielectric (theoretically absorption-free) back reflectors is a key topic.

In this article three novel light-trapping techniques for manipulating light inside solar cells are presented. The first technique deals with the manipulation of light scattering at rough interfaces inside a solar cell. The surface texture of these rough interfaces is so designed that light is scattered into (pre) selected angles. We shall refer to this approach as the **angle-selective** management of scattered light at surface-textured interfaces. The second technique treats the **modulated surface textures**, which are a combination of large and small surface features of substrate carriers. The modulated surface-texture substrates allow light scattering in a broader range of wavelengths. The third technique deals with the manipulation of reflection and transmission at a particular interface inside a solar cell. This specially designed *optical interface* results in a **wavelength-selective** management of (high) reflection or transmission of light. In this article the periodically-designed surface textures, such as periodic gratings, are representatives of the first technique, textured glass substrates coated with an etched aluminum-doped zinc oxide (AZO) are examples of the modulated surface textures, and the one-dimensional (1-D) photonic-crystal-like (PC) structures are introduced as the *optical interfaces* for the realization of the third technique.

3.1   1-D periodic diffraction gratings

Diffraction gratings were introduced into thin-film solar cells in order to achieve better control of light scattering inside the cells. The switch from randomly-textured surfaces to 1-D periodic gratings allows to suppress the total reflection in the wavelength region of interest and to scatter light into (pre) selected angles by manipulating geometrical parameters P and h of the gratings /3//7/. Figure 4 shows the surface morphology of a periodic grating patterned in a lacquer on glass substrate that was characterized by Atomic Force Microscopy (AFM).
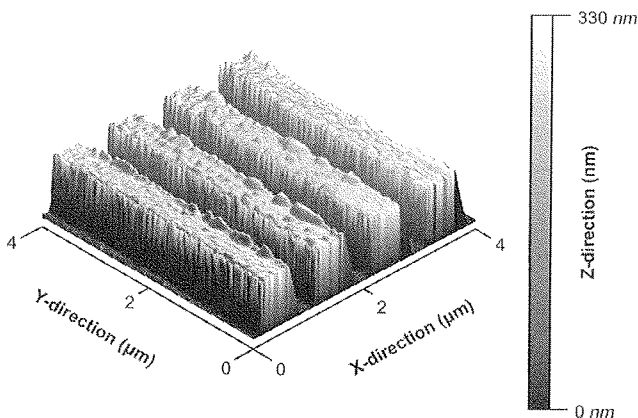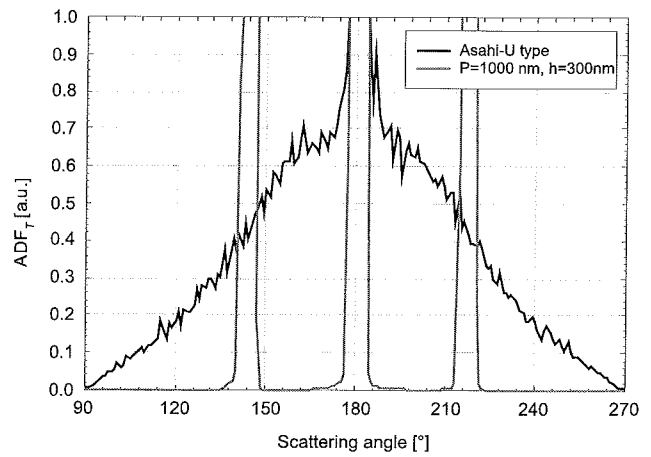

Fig. 4:   3D-view of a grating with P = 1000 nm and
h = 300 nm.

Fig. 5:   ADF_T (at 633 nm) of Asahi-U type substrate and
grating (P = 1000 nm and h = 300 nm).

The understanding of scattering properties of 1-D gratings is important in order to make a right choice of the P and h for the use in a particular solar cell. The scattering properties are described by the angular distribution function (ADF) and the haze in transmission for 1-D grating. In Figure 5 the ADF_T of the 1-D periodic grating and of the Asahi-U type substrate are shown. The measurement confirmed that light was scattered into selected angles from the 1-D periodic gratings according to the diffraction grating equation:

$$\varphi_{scatt} = \arcsin\left[\frac{m\lambda}{nP} - \sin(\varphi_{inc})\right] \qquad (1)$$

Furthermore Fig. 5 demonstrates the fundamental difference in the ADF between randomly surface-textured substrate, such as Asahi-U type substrate, and 1-D periodic gratings. In case of randomly surface-textured substrates the ADF is a continuous function of the scattering angle, while in case of periodic gratings the light is scattered into discrete angles.

The haze in transmission of 1-D gratings that had different P and constant h is shown in Fig. 6. Also for this scattering parameter the geometrical features P and h play an important role, as the value of P represents the threshold for scattering the light (according to Equation 1, for λ > P diffraction modes are not allowed, therefore only specular component may be transmitted) and h is directly related to the value of the haze (for h aiming to zero the 1-D grating approximates a flat surface) /14/.

Although some theoretical questions regarding 1-D gratings are still open, such as the relationship between the intensity of diffraction modes and h and knowledge of the scattering properties in different media than glass/air, 1-D gratings have been already successfully used as scattering surfaces in thin-film silicon solar cells in both superstrate /14/ and substrate configuration /15/.
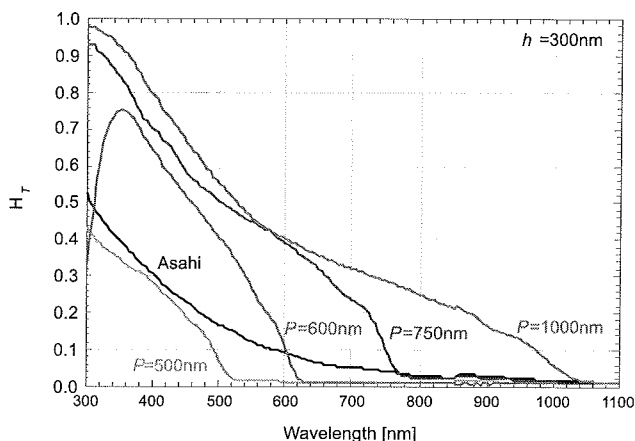
Fig. 6: Haze in transmission of gratings with different period and constant height (h = 300 nm). Asahi-U type is present as reference for randomly-textured surfaces (exponential decay).

3.1.1 Solar cell on 1-D periodic grating

As an example of the scattering potential of 1-D periodic surface texture in solar-cell technology, a p-i-n thin-film a-Si:H solar cell deposited on glass with 1-D periodic grating (P = 600nm and h = 300 nm) is presented. A 1000 nm thick ZnO:Al layer as the front contact was deposited on the textured glass substrate using the RF magnetron sputtering. The solar cell was fabricated using rf-PECVD deposition technique and its structure was: glass / fron ZnO:Al / p-layer (mc-Si:H) / p-layer (a-SiC:H) / buffer layer (a-SiC:H) / i-layer (a-Si:H) / n-layer (a-Si:H) / Ag / Al. The change of the surface roughness was evaluated using AFM after the deposition of each layer. The initial periodicity was preserved up till the back contact, although the height of the periodic structure decreased after the deposition of each subsequent layer. The external parameters of the solar cell are reported in Table 1 and compared with those of solar cells deposited on Asahi-U type and flat ZnO:Al as references. In Figure 7 the external quantum efficiency (EQE) of the compared solar cells is reported.

Table 1: Initial external parameters of solar cells.

Texture	V_{OC} [V]	J_{SC} [mA/m²]	FF	η [%]
Asahi-U	0.845	-15.2	0.708	9.09
Flat	0.849	-13.4	0.641	7.29
P600 x h300	0.833	-14.8	0.707	8.7

The difference in J_{SC} between the solar cells deposited on the 1-D grating and the Asahi-U type substrate can be mainly explained by the higher absorption in the short wavelength region in the ZnO:Al compared to the SnO₂:F front contacts. For wavelengths above 500 nm, the EQE of the solar cell deposited on the grating is higher than the EQE of the solar cell deposited on the flat substrate. Due to anti-reflective and scattering effects, the EQE in this wavelength region is similar to Asahi-U reference.
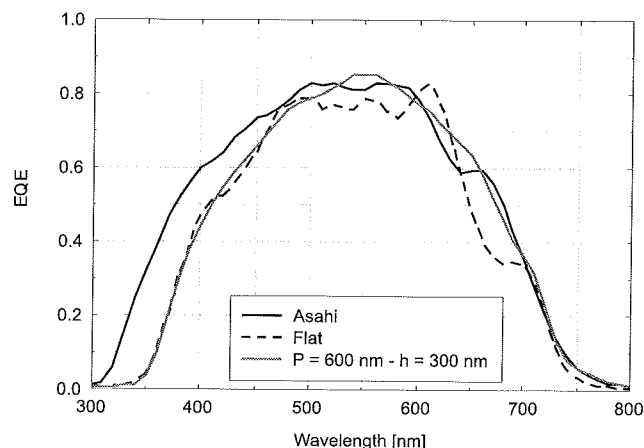

Fig. 7: The EQE of the compared solar cells.

This result indicates that 1-D periodic gratings are suitable substrates for improved light management in thin-film silicon solar cells. 1-D gratings were fabricated in several combinations of period and height on glass substrates and use as substrates for a-Si:H solar cells. High performance was obtained in solar cells with diffraction grating substrates having P = 600 nm and h = 300 nm. The J_{SC} of this solar cell increased by 14.2% relative to the J_{SC} of the solar cell with flat interfaces.

3.2 Modulated surface textures

The term modulated texture refers to a surface morphology that combines two types of textures with different statistical (vertical and lateral) surface parameters. This concept aims at enhanced light scattering in a broader wavelength range combining large and small surface features. This approach is an interesting choice for surface texturing in tandem thin-film silicon solar cells. In this article one example of modulated surface texture is presented: a combination of (large) random and (small) random textures. The different textures were introduced at different interfaces of the substrate, namely large random features were introduced at the glass / ZnO:Al interface and small random features were created at the ZnO:Al / air interface. The large random surface texture was obtained by treating flat Corning Eagle 2000™ glass in a compound solution composed of HF and H₃PO₄ for 35 minutes. A 1 mm thick ZnO:Al film was sputtered on top of the rough glass surface. The modulated surface texture was obtained by wet-etching of the ZnO layer for 40".

3.2.1 Analysis of the modulated textures

The AFM was intensively used to evaluate the development of the modulated textures since it delivered highly detailed images and statistical information of the surface. An initial decrease in the surface roughness was measured after the deposition of the ZnO:Al mainly due to the smoothening effect. After the etching of the ZnO:Al layer the surface roughness increased resulting in the superimposition of the large and small features on the same surface. The im-

age of the modulated surface texture on etched glass in Fig. 8 shows clearly the combination of large features (away from each other in the order of microns) with smaller holes and craters (fingerprint of the etched AZO 40").

A simple and comprehensive means to represent the surface modulation is the spatial-frequency surface representation /16/. Using this representation the discrete lateral features that dominate the vertical surface roughness can be evaluated. It also helps to understand why surface profiles with similar mean-square-root surface roughness may have different scattering behavior. When comparing the spatial-frequency surface representations of the etched glass and its modulated version (etched glass + etched AZO) one can observe in both cases the broad peak at low spatial-frequency components that correspond to the large features. In the case of modulated surface texture the high spatial-frequency components (small holes and craters) are present in the spatial-frequency representation that are a consequence of the etching of ZnO:Al layer.

The haze parameter of the modulated surface textures is presented in Fig. 9. The initial textured surface exhibited low scattering level due to the large features. The surface covered with the ZnO:Al showed a similar behavior as the bare surface. Regarding the modulated textures, the haze values were boosted because of the etching step that provided additional rough features.

3.2.2 Solar cells on modulated surface textures

Single junction a-Si:H p-i-n solar cells were deposited by rf-PECVD on the modulated surface-textured susbtrates. The back contact consisted of a thin layer of ZnO:Al (80 nm) and silver. An overview of the initial external parameters is reported in Table 2. The EQE of the a-Si:H cells deposited on the modulated surface-textured substrate is shown in Figure 10.

The spectral response of the solar cells deposited on modulated surface textures was improved in the short wavelength region with respect to the solar cells deposited either on AZO 40" substrate or on etched glass covered by the ZnO:Al layer. This enhancement results partly from the different thickness of the ZnO:Al layer before and after etching and partly on the anti-reflecting (AR) effect of the modulated surface texture.

Table 2: *Initial external parameters of solar cells deposited on modulated surface textures.*

Texture	V_{OC} [V]	J_{SC} [mA/cm^2]	FF	η [%]
Etched glass/AZO 40"	0.874	17.8	0.639	9.97

The high surface roughness of the modulated texture and its corresponding spectral-frequency distribution, which affects the scattering and AR properties, led to the high EQE in the long wavelengths region. This result demonstrates the potential of modulated surface-textured sub-
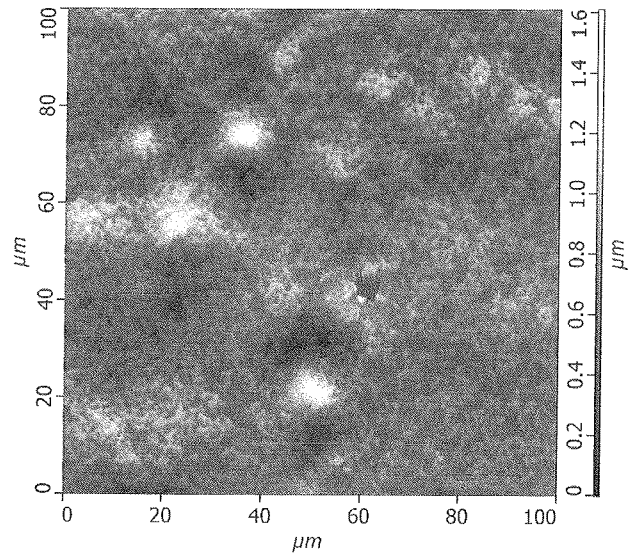

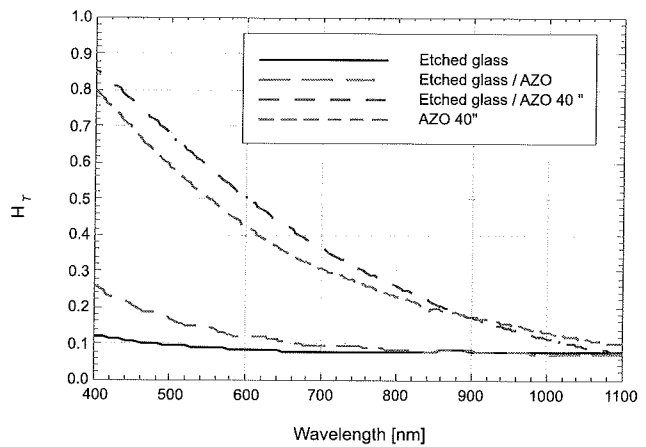Fig. 8: Top view of the modulated surface texture on etched glass.

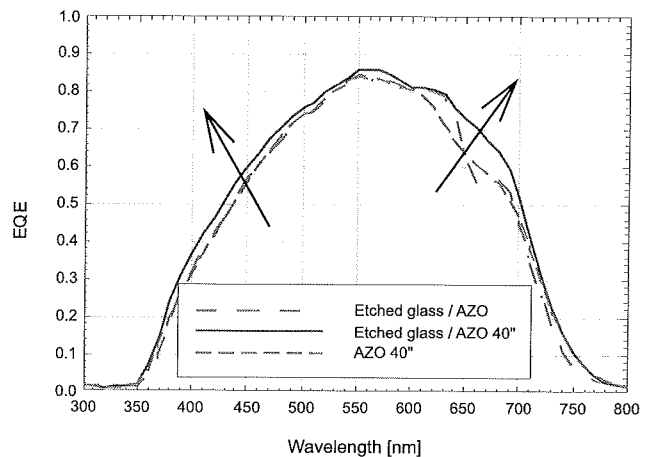Fig. 9: Haze parameter in transmission of the substrates with the texture types (b).

Fig. 10: EQE of the solar cells deposited on different surface-textured substrates.

strates for enhancing the absorption of light in the absorber layers of thin-film silicon solar cells.

3.3 1-D photonic-crystal-like structures as distributed Bragg reflector

Optical losses can occur at the metallic back contact of thin-film silicon solar cells because the surface-textured silver back reflectors suffer from undesired plasmon absorption /17/. In order to minimize such losses in single or tandem silicon solar cells an optimal approach for engineering a high-quality back reflector is desired. The design of such back reflector has to result in a high reflectance at the back contact in the solar cell in a broad and tunable wavelength region. These design specifications match the behavior of 1-D PC in the role of distributed Bragg reflector (DBR). 1-D PC is a multilayer structure in which two layers with different optical properties (refractive indexes) are periodically alternated. When light propagates through this structure, constructive and deconstructive interferences arise, resulting in the wavelength-selective reflectance or transmittance behavior. It has been demonstrated that periodically repeated stacks of a-Si:H and a-SiN$_x$:H (deposited using rf-PECVD at 235 °C) on glass exhibit a highly-reflective behavior in a broad range of wavelengths /18/. Operational 1-D PCs were fabricated on thin-film silicon compatible substrates (glass / etched ZnO:Al) and at compatible temperature < 180 °C /19/. The effects of the deposition temperature, the different substrate (from flat glass to glass/etched ZnO:Al), and the angle of incidence on the optical properties of 1-D PCs were determined. The high reflectance (80-90%) achieved in a broad wavelength region of 400 nm was in good agreement with the simulations of these structures.

3.3.1 Solar cells with DBR

Three pairs of layers of a-Si:H and a-SiN$_x$:H were used to fabricate an 1-D PC operational as the DBR. The schematic structure of the solar cell is given in Fig. 11. The structure consisted of glass coated with rough front ZnO:Al layer, a typical single-junction thin-film silicon p-i-n solar cell, a 700 nm thick ZnO:Al film used as back electrode. Three different back reflectors were applied at the back side of the solar cell, namely ZnO:Al / air (reference), ZnO:Al / Ag, and ZnO:Al / 1-D PC (see Figure 11).

The measured EQE of solar cells with different back reflectors is presented in Fig. 12. The EQE did not show the state-of-the-art performance because of some processing issues. Additionally, a high absorption in ZnO:Al front contact could be responsible for a low response in the short-wavelength region. The EQE increased in the long-wavelength region where the positive effect of the back reflectors was expected. The trend of increasing EQE is visualized by the arrows in the plot. In case of the textured metallic back reflector, surface plasmon absorption was responsible for a lower EQE in comparison with the 1-D PC back reflector, where the plasmon absorption was not expected.
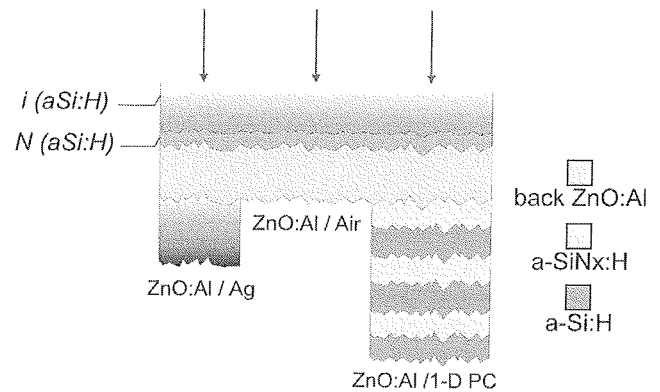

Fig. 11: Zoom-in at back side of the solar cell provided with three different back reflectors (the three red arrows indicate the place where the beam of EQE setup is directed).
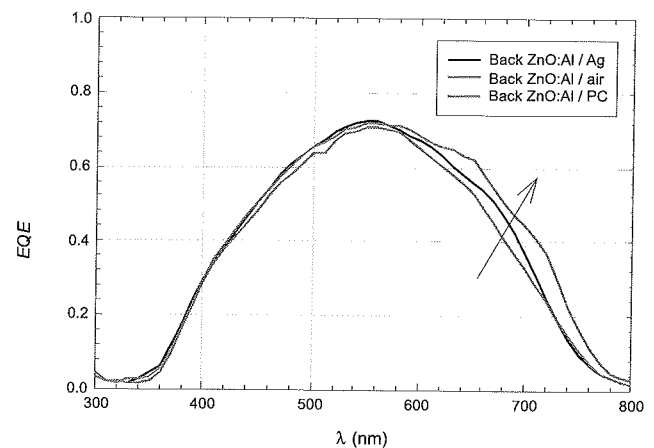

Fig. 12: EQE of solar cells on rough front ZnO:Al stacked with different back reflectors.

4 Conclusion

Approaches to improve the stability of a-Si:H solar cell against light-induced degradation and to enhance the absorption in absorber layers of thin-film silicon solar cells were presented.

Dilution of the silane source gas with hydrogen during the PECVD deposition of silicon films results in interesting modifications of the structural properties of the films in reference to undiluted ones. Although the phase transition is the most evident effect of the hydrogen dilution, more subtle changes do also occur in the amorphous silicon. The detailed XRD analysis of the pc-Si:H films revealed a narrowing of the FSP of the XRD patterns with increasing hydrogen dilution. The most important result from the XRD analysis of the pc-Si:H films is the presence of ordered domains of tetragonal silicon hydride in the films. A degradation experiment demonstrated the improved stability of the cells with absorber layers prepared at higher hydrogen dilution. However, the degradation of solar cells with absorber layers prepared at R > 20 is not further reduced with a

further increase of R. This result indicates that there is a strong link between the degradation behavior of the solar cells and the medium range order of the individual films (estimated from the FSP width of the XRD pattern), which also saturates for films prepared at R > 20.

There are several novel approaches to light trapping techniques such as the use of 1-D periodic gratings, modulated surface-texture substrates and design and implementation of distributed Bragg reflectors based on dielectric films. The gratings were successfully employed in single junction a-Si:H solar cells. High performance was obtained on solar cells using diffraction grating with P = 600 nm and h = 300 nm, where J_{SC} of this solar cell increased by 14.2% relative to the J_{SC} of the solar cell with flat interfaces. The concept of modulated surface texture and the spatial-frequency surface representation of the surface were presented. Solar cells deposited on modulated surface-textured ZnO:Al/glass substrate exhibited higher EQE in comparison to a solar cell deposited on surface-textured ZnO or glass due to improved anti-reflective and scattering properties of rough interfaces. 1-D PC can be used to obtain high reflectance at the back contact in a broad and tunable wavelength region. 1-D PCs based on a-Si:H and a-SiN$_x$:H layers were designed by computer simulations, fabricated and implemented in a-Si:H solar cells. The use of 1-D PC back reflector resulted in a higher EQE in the long-wavelength region in comparison to other types of back reflectors. The absence of absorption losses in the dielectric layers of 1-D PC makes the combination of ZnO:Al / PC a good candidate for back reflectors.

Acknowledgments

References

/1/ W. Spear and P. LeComber,Solid State Comm. 17 (9), 1193 (1975).

/2/ D.E. Carlson and C.R. Wronski, Appl. Phys. Lett. 28 (11), 671 (1976).

/3/ J. Meier et al., in Proc. of the 1st World Conference on Photovoltaic Energy Conversion, Hawai (1994), p. 409-412.

/4/ J. Yang, A. Banerjee, K. Lord, and S. Guha, in Proc. of the 2nd World Conference and Exhibition on Photovoltaic Solar Energy Conversion, Vienna (1998), p. 387-390.

/5/ Photon International, March 2009.

/6/ L. Yang and L. F. Chen, Mater. Res. Soc. Proc. 336 (1994) 669.

/7/ J. Yang, X. Xu and S. Guha, Mater. Res. Soc. Proc. 336 (1994) 687.

/8/ C.R. Wronski, J.M. Pearce, R.J. Koval et al., Mater. Res. Soc. Proc. 715 (2002) A13.4.

/9/ G. van Elzakker, V. Nádaždy et al., Thin Solid Films 511-512 (2006) 252-257.

/10/ G. van Elzakker, P. Sutta, M. Zeman, Mater. Res. Soc. Symp. 1153 (2009) 1153-A18-02.

/11/ D.L. Williamson, Mater. Res. Soc. Symp. Proc. 559 (1999) 251.

/12/ S. Minomura, K. Tsuji et al., Journal of Non-Cryst. Solids 35&36 (1980) 513-518.

/13/ C. C. Tsai, G. B. Anderson, R. Thompson et al., Journal of Non-Cryst. Solids 114 (1989) 151.

/14/ O. Isabella et al., in Proc. of the 23rd EUPVSEC, Valencia (2008), 3AV.1.48.

/15/ F.-J. Haug et al., in Proc. of teh 21st EUPVSEC, Dresden, (2006).

/16/ O. Isabella et al., in Proc. of the 23rd ICANS, Utrecht, (2009).

/17/ J. Springer, A. Poruba, L. Mullerova, et al., , J. Appl. Phys. 95, 1427 (2004).

/18/ J. Krc, A. Campa, S. Luxembourg, M. Zeman and M. Topic, Mater. Res. Soc. Symp. Proc. 1101E, (2008), 1101-KK08-01.

/19/ O. Isabella, B. Lipovsek, J. Krč, M. Zeman, Mater. Res. Soc. Symp. Proc. 1153 (2009), 1153-A03-05.

M. Zeman, G. van Elzakker, O. Isabella
Delft University of Technology, PVMD /DIMES,
Feldmannweg 17, 26282 CT Delft, Netherlands

P. Sutta
University of West Bohemia, NTRC,
Univerzitní 8, 306 14 Plzeň, Czech Republic

J. Krc
University of Ljubljana, Faculty of Electrical
Engineering, SI-1000 Ljubljana, Slovenia
janez.krc@fe.uni-lj.si